JOURNAL OF BACTERIOLOGY, Mar. 2005, p. 1659–1667 Vol. 187, No. 5
0021-9193/05/$08.00+0 doi:10.1128/JB.187.5.1659–1667.2005

Genomic Analysis of Anaerobic Respiration in the Archaeon *Halobacterium* sp. Strain NRC-1: Dimethyl Sulfoxide and Trimethylamine *N*-Oxide as Terminal Electron Acceptors†

Jochen A. Müller and Shiladitya DasSarma*

Center of Marine Biotechnology, University of Maryland Biotechnology Institute, Baltimore, Maryland

Received 12 October 2004/Accepted 6 December 2004

We have investigated anaerobic respiration of the archaeal model organism *Halobacterium* sp. strain NRC-1 by using phenotypic and genetic analysis, bioinformatics, and transcriptome analysis. NRC-1 was found to grow on either dimethyl sulfoxide (DMSO) or trimethylamine *N*-oxide (TMAO) as the sole terminal electron acceptor, with a doubling time of 1 day. An operon, *dmsREABCD*, encoding a putative regulatory protein, DmsR, a molybdopterin oxidoreductase of the DMSO reductase family (DmsEABC), and a molecular chaperone (DmsD) was identified by bioinformatics and confirmed as a transcriptional unit by reverse transcriptase PCR analysis. *dmsR*, *dmsA*, and *dmsD* in-frame deletion mutants were individually constructed. Phenotypic analysis demonstrated that *dmsR*, *dmsA*, and *dmsD* are required for anaerobic respiration on DMSO and TMAO. The requirement for *dmsR*, whose predicted product contains a DNA-binding domain similar to that of the Bat family of activators (COG3413), indicated that it functions as an activator. A cysteine-rich domain was found in the *dmsR* gene, which may be involved in oxygen sensing. Microarray analysis using a whole-genome 60-mer oligonucleotide array showed that the *dms* operon is induced during anaerobic respiration. Comparison of *dmsR*$^+$ and Δ*dmsR* strains by use of microarrays showed that the induction of the *dmsEABCD* operon is dependent on a functional *dmsR* gene, consistent with its action as a transcriptional activator. Our results clearly establish the genes required for anaerobic respiration using DMSO and TMAO in an archaeon for the first time.

Extremely halophilic archaea (haloarchaea) generally grow heterotrophically under aerobic conditions in hypersaline environments, although they possess facultative anaerobic capabilities (9). These anaerobic capabilities are important since the high salt concentrations and elevated temperatures the organisms encounter, together with high cell densities promoted by aerobic growth and flotation, reduce the availability of molecular oxygen. Although haloarchaeal microorganisms frequently encounter microaerobic or even anoxic conditions, detailed knowledge regarding the extent of haloarchaeal anaerobic growth is still only beginning to emerge. Some species of haloarchaea can carry out primary energy conservation in the absence of molecular oxygen via photophosphorylation (13), substrate-level phosphorylation (13), and anaerobic respiration using nitrate (references 9 and 42 and references therein). In addition, two previous reports described the ability to use dimethyl sulfoxide (DMSO) and trimethylamine-*N*-oxide (TMAO) (23), and to some extent fumarate (22), as alternative electron acceptors for growth enhancement for some haloarchaea.

The molecular basis of the DMSO and TMAO respiratory systems has not been described for any member of the domain *Archaea*. By contrast, in various bacterial model organisms, DMSO reductases and the related TMAO reductases are well characterized as membrane-bound or periplasmic terminal reductases forming dimethyl sulfide or trimethylamine, respectively, as the final product (7, 17, 19, 29, 30, 32, 39). In *Escherichia coli*, the molecular components of the DMSO reductase are DmsA, the catalytically active subunit harboring molybdenum-molybdopterin (MPT) as a cofactor; DmsB, a subunit containing iron-sulfur clusters for electron transport; DmsC, a membrane anchor; and DmsD, a molecular chaperone. Other bacterial DMSO and TMAO reductases may contain a membrane-bound *c*-type cytochrome (DorC or TorC) instead of DmsB and DmsC (17, 31, 32). The expression of the corresponding *dms* and *tor* genes in bacteria may be regulated by a two-component regulatory system (e.g., TorR-TorS) (15, 33) or the global oxygen response regulator FNR (6). Additional regulation may be provided by the presence of the preferred terminal electron acceptor nitrate or the absence of molybdenum (1, 6).

In the present study, we describe the first functional genomic characterization of the DMSO/TMAO respiratory system in the haloarchaeal model organism *Halobacterium* sp. strain NRC-1. Previous annotation reported a single *dmsA* gene surrounded by additional, unspecified MPT oxidoreductase genes (20). Reexamination of the *dmsA* region, in this investigation, found a total of six genes, *dmsREABCD*, forming an operon that functions as the DMSO/TMAO respiration system (Fig. 1). Here, we report a combination of genetic and transcriptional data that establish the requirement for the *dmsREABCD*

* Corresponding author. Mailing address: Center of Marine Biotechnology, University of Maryland Biotechnology Institute, 701 E. Pratt St., Suite 236, Baltimore, MD 21202. Phone: (410) 234-8847. Fax: (410) 234-8896. E-mail: dassarma@umbi.umd.edu.

† Supplemental material for this article may be found at http://jb.asm.org/.

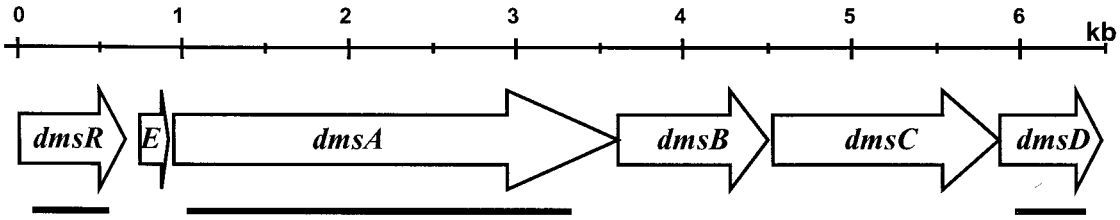

FIG. 1. Physical map of the *dms* gene locus in *Halobacterium* sp. strain NRC-1. The locations and directions of open reading frames are indicated by arrows. Regions of *dmsR*, *dmsA*, and *dmsD* deleted in *Halobacterium* sp. strains JAM101, -102, and -103 are indicated by horizontal bars.

operon of *Halobacterium* sp. strain NRC-1 for anaerobic respiration, utilizing DMSO and TMAO, in an archaeon.

MATERIALS AND METHODS

Strains, plasmids, and growth conditions. *Halobacterium* sp. strain NRC-1 was grown in complex medium containing peptone (10 g/liter) and 10 mM citrate (CM^+ medium) (10) either under aerobic conditions or under anaerobic conditions in the presence of an alternative electron acceptor. For anaerobic growth, the medium was kept in an anaerobic glove box (Coy Laboratory Products, Ann Arbor, Mich.) with an N_2-H_2 (95:5 [vol/vol]) atmosphere for 1 day prior to inoculation. The medium contained the redox indicator resazurin to test for anoxic conditions. Even without added reducing agent, the pink color of oxidized resazurin disappeared in sterile, freshly prepared CM^+ medium when kept overnight under an oxygen-free atmosphere. This was likely due to reduction of resazurin to the colorless form by redox-active components, e.g., cysteine, in the medium. The cultivation vessel containing the medium was sealed inside the anaerobic chamber with a butyl rubber stopper, and an electron acceptor (TMAO or DMSO) was added from a sterile stock solution. Cultivation vessels were shaken at 220 rpm at 42°C in the dark. Growth was monitored spectrophotometrically by determining the optical density at 600 nm. The concentration of dimethyl sulfide during growth on DMSO was quantified by gas chromatography (18). The presence of trimethylamine during growth on TMAO was detected by its characteristic odor. All cultivation experiments were performed at least in triplicates.

E. coli strain DH5α was used as a host for cloning vectors. The strain was grown in Luria-Bertani medium at 37°C, and ampicillin was added at 50 μg/ml when appropriate. The strains and plasmids used in this study are listed in Table 1.

DNA isolation and PCR amplification. Standard protocols were used for DNA cloning and transformation into *E. coli* (27). Chromosomal DNA of strain NRC-1 was isolated as described previously (10). Purifications of PCR products, DNA fragments from restriction enzyme digests, and plasmids were performed with Qiaprep spin colums (Qiagen). PCR mixtures contained 100 ng of genomic DNA, a 200 nM concentration of each primer, 200 μM deoxynucleoside triphosphates, and 1 U of *Taq* polymerase (Promega) in PCR buffer with 1.5 mM $MgCl_2$. PCR parameters were as follows: 3 min at 92°C; 30 cycles of 1 min at 94°C, 1 min at 60°C, and 1 min at 72°C; and 5 min at 72°C.

Construction of deletion mutants. A vector, plasmid pJAM10, was constructed for gene deletion in strain NRC-1 in combination with blue-white screening in *E. coli*. A 1.3-kb DNA fragment containing the *Halobacterium* sp. strain NRC-1 *ura3* gene including 500 bp of the 5′ flanking DNA sequence regions was amplified with *Pfu* (Stratagene) and the primers ura3F (5′-AGGAGGCGTGCTG GAATGGTCGCT-3′) and ura3R (5′-GGGCCGCCGGCTGACTACCCG-3′). This PCR fragment was cloned into pUC19 digested with SspI.

For deletion of *dmsR* (VNG826), plasmid pJAM101 was generated. First, a 463-bp DNA fragment containing the 5′ region of *dmsR*, including 421 bp of 5′ flanking DNA sequence, and a 510-bp DNA fragment containing the 3′ region of *dmsR*, including 497 bp of 3′ flanking DNA sequence, were PCR amplified with primers dmsR5_F_Xba (5′-GCTCTAGACCACGACCGGCTCCCCAACC-3′) and dmsR5_R_Eco (5′-CGGAATTCACGAGCCCCACGAGCAGTAG-3′) and primers dmsR3_F_Eco (5′-CGGAATTCCAACACGCCGGACGCACAC GAG-3′) and dmsR3_R_Xba (5′-CCTCTAGAGGCGAGCAGGCGGTTTTG ACGAC-3′), respectively. Both fragments were digested with EcoRI, purified, and ligated. The ligated fragment was digested with XbaI, purified, and cloned into pJAM10 cut with XbaI. The correct incorporation of the 5′ and 3′ DNA sequence regions of *dmsR* into pJAM10 was verified by PCR analysis. Plasmid pJAM101 resulted in an in-frame deletion of codons 14 to 211 of *dmsR* (absolute positions 626492 to 627094). The plasmids pJAM102 for deletion of *dmsA* (with the primers dmsA5_F_Xba [5′-GCTCTAGACGACGGCGCTTGGCATCT-3′], dmsA5_R_Eco [5′-CGGAATTCCCGGGTGGCGTTGAGGTC-3′], dmsA3_F_Eco [5′-CGGAATTCCCCCGCCTGCGTCGTGAACTGTCC-3′], and dmsA5_R_Xba [5′-GCTCTAGAGGGGCGGCGTGCGGTCGTGTCG-3′]) and pJAM103 for deletion of *dmsD* (VNG832) (with the primers dmsD5_F_Xba [5′-GCTCTAGAT CGTCGCGCCCGTGTTCAT-3′], dmsD5_R_Eco [5′-CGGAATTCCGCGCT GCAGGGGGAGATAG-3′], dmsD3_F_Eco [5′-CGGAATTCACGCCGTCTC CAGCAGTCA-3′], and dmsD3_R_Xba [5′-CGTCTAGACGCCATCCGGTCT TTGTA-3′]) were generated in an analogous manner. Plasmid pJAM102 resulted in an in-frame deletion spanning the region between codons 10 and 808 of *dmsA* (absolute positions 627475 to 629869), and plasmid pJAM103 resulted in an in-frame deletion between codons 9 and 183 of *dmsD* (absolute positions 632074 to 632597).

TABLE 1. Strains and plasmids used in this study

Strain or plasmid	Characteristics	Source (reference)
Halobacterium sp. strains		
NRC-1	Wild type	Laboratory collection (28)
SK400	NRC-1 Δ*ura3*	Laboratory collection (31)
JAM101	SK400 Δ*dmsR*	This study
JAM102	SK400 Δ*dmsA*	This study
JAM103	SK400 Δ*dmsD*	This study
E. coli strain DH5α	*supE44* Δ*lacU169* ϕ80Δ*lac*ZM15 *hsdR17 recA1 endA1gyrA96 thi-1 relA1*	Invitrogen
Plasmids		
pUC19	Cloning vector, *lacZ bla*	New England Biolabs
pJAM10	pUC19 containing NRC-1 *ura3* with flanking region	This study
pJAM101	pJAM10 containing truncated *dmsR* with flanking region	This study
pJAM102	pJAM10 containing truncated *dmsA* with flanking region	This study
pJAM103	pJAM10 containing truncated *dmsD* with flanking region	This study

Transformation of *Halobacterium* sp. strain NRC-1 Δ*ura3*, a uracil auxotroph, with plasmid pJAM101, pJAM102, or pJAM103 was carried out essentially as described previously (24, 37). In brief, first-crossover integrants were obtained by using uracil-deficient medium. The integration of plasmid was confirmed by screening for the presence of the *ura3* gene. Second-crossover recombinants were selected for on rich CM^+ plates in the presence of 0.25 mg of 5-fluoro-orotic acid (Toronto Research Chemicals) per ml. Recombinants were screened by PCR to confirm loss of the *ura3* gene and for the presence of either the deletion or wild-type target gene.

RT-PCR. Total RNA was prepared from DMSO-grown strain NRC-1 cells in mid-log phase. Cells were harvested by centrifugation of the culture (8,000 × *g*, 5 min, 2°C) in chilled beakers. RNA was isolated immediately after cell harvest by using spin columns (Agilent, Palo Alto, Calif.). Lysis of cells was carried out directly in lysis buffer. Two treatments with DNase (Invitrogen) were carried out in order to remove contaminating DNA from the RNA preparations. Synthesis of cDNA was done from 500 ng of RNA and 2 pmol of specific primer with SuperScript II RNase H^- reverse transcriptase as described by the supplier (Invitrogen). For amplification of parts of *dmsR* and intergenic regions of *dmsR* and *dmsA*, *dmsE* and *dmsA*, *dmsA* and *dmsB*, *dmsB* and *dmsC*, and *dmsC* and *dmsD*, six sets of primers were chosen for reverse transcriptase PCR (RT-PCR): dmsRf (5′-AGCGCACAGCCAGCCAGCCGAACA-3′) and dmsRr (5′-CGAG CCGCGTCAGGTGGGTCAGC-3′), i-dmsRf (5′-GATGCTCGCGGACTGTG GCTACG-3′) and i-dmsAr (5′-CGCGCTGATCGGGCTGTGG-3′), i-dmsEf (5′-CCAACACGCCGGACGCACACGAG-3′) and i-dmsAr (5′-GGCGAGCA GGCGGTTTTGACGAC-3′), i-dmsAf (5′-ACTTCGTCGACGGGCACCTCC AG-3′) and i-dmsBr (5′-CGTTCACCGGGCAGACCTTCACAC-3′), i-dmsBf (5′-CGGACGCCCCTGGAAGAGCAAGAA-3′) and i-dmsCr (5′-CAACAGC CCCGCGACGATGATG-3′), and i-dmsCf (5′-AGTACGCCGGCCTCACGA C-3′) and i-dmsDr (5′-TCCGGGCCCGACGAACAGT-3′). The PCR amplifications were done by using 1 U of *Taq* polymerase and standard conditions (30 cycles). Negative controls without reverse transcriptase to test for absence of genomic DNA in the assay were included.

Microarray design. Oligomer (60-mer) probes were designed for 2,473 open reading frames (ORFs) of *Halobacterium* sp. strain NRC-1 by using the program OligoPicker (38). Up to three probes were designed per gene. Duplicate genes were considered only once for probe design. A BLAST search of all probes against the genome of *Halobacterium* sp. strain NRC-1 was carried out in order to ensure specificity. The melting temperature range of the probes was 3°C, with a mean melting temperature of 81°C. Microarray slides were fabricated by in situ oligonucleotide synthesis (Agilent) (14). The slides harbor 8,455 features per array, with two arrays per slide. The features include the gene probes (8,077), present randomly and often in multitude (the average occurrence of probes is 1.4 times), as well as negative and positive control spots to test hybridization conditions. Sequences of 364 control spots were designed by Agilent; sequences for additional 14 control spots were taken from the genomes of *Mycobacterium tuberculosis* (65.6% GC content) and *Mycobacterium leprae* (57.8% GC content), both of which have percent GC contents comparable to those of *Halobacterium* sp. strain NRC-1 genetic elements.

Microarray analysis. *Halobacterium* sp. strain NRC-1 was grown under aerobic conditions and anaerobic conditions, using TMAO as an electron acceptor, to early exponential growth phase (optical density at 600 nm of 0.15 to 0.3). Cultivation of cells (50 ml) was carried out in 500-ml flasks to ensure proper mixing of culture fluid. Cells were harvested by chilling the incubation vessels in an ethanol-dry ice bath for 1 min followed by centrifugation of the culture (8,000 × *g*, 5 min, 2°C) in chilled beakers. Total RNA was isolated as described above. DNA was hydrolyzed in RNA preparations with DNase (Invitrogen). For cDNA synthesis, RNA preparations from three cultures grown under identical conditions were pooled to equal parts in order to minimize biological noise. Fluorescently labeled cDNA was prepared essentially as described by M. Laub et al. (http://caulobacter.stanford.edu/CellCycle/protocols.htm). In brief, 7 μg of total RNA was combined with 500 ng of random hexamers (Qiagen) and reverse transcribed to Cy3- or Cy5-dCTP (Amersham Pharmacia)-labeled cDNA by using SuperScript II RNase H^- reverse transcriptase (Invitrogen). Subsequently, the cDNA preparations were purified after alkaline hydrolysis of RNA at 65°C with Qiagen spin columns. To control for labeling differences, duplicate reactions in which the Cy3 and Cy5 labels were switched during synthesis were carried out. The labeled cDNA targets were mixed with hybridization buffer (Agilent) and control targets (Agilent) and hybridized to microarray slides, assembled into a hybridization chamber (Agilent), for 17 h at 60°C in the dark. After hybridization, the slides were washed in 6× SSC (1× SSC is 0.15 M NaCl plus 0.015 M sodium citrate)–0.005% Triton X-102 for 10 min at room temperature followed by 0.1× SSC–0.005% Triton X-102 for 5 min at 4°C. The microarray slides were scanned for the Cy3 and Cy5 fluorescent signals with an Agilent DNA microarray scanner (model no. G2565BA).

Image processing and statistical analysis were carried out with Agilent Feature Extraction software, version 7.1. Spot signal intensities were adjusted by subtracting local background, and a two-sided *t* test was performed to assess whether the signal was significantly different from the background signal. Fluorescence intensities were normalized by using the LOWESS method (5). Log ratios for each feature were calculated from the processed red and green signals. The significance of the log ratio was assessed by computing the most conservative log ratio error and significance value (*P* value), using a standard error propagation algorithm (Agilent) and a universal error model (Rosetta Biosoftware). After removal of outliers, the final log ratio, fold change of gene expression, log ratio error, and *P* value for a gene were calculated as arithmetic means of all probe values for that gene.

Computational analysis of DNA and amino acid sequences. BLAST analysis and sequence manipulation were done with the bioinformatics tools available on our server and website (http://zdna2.umbi.umd.edu). Sequence data were obtained either from our website or from the National Center for Biotechnology Information. Nucleotide and amino acid sequence analyses were performed with the programs from the Wisconsin Genetics Computer Group software package (Accelrys, San Diego, Calif.), the DNAStar (Madison, Wis.) software package, Clustal_X (version 1.81), and Simple Modular Architecture Research Tool SMART (http://smart.embl-heidelberg.de). Phylogenetic analysis for Dms proteins was performed with Clustal_X for multiple-sequence alignment together with Treeview for neighbor-joining tree construction (34), as well as Treepuzzle (http://www.nsc.liu.se/software/biology/puzzle5).

RESULTS

Characterization of *Halobacterium* sp. strain NRC-1 anaerobic respiration using DMSO and TMAO. Some enhancement of anaerobic growth of strain NRC-1 with DMSO and TMAO as terminal electron acceptors has been reported before (23). Since details were not published, we reinvestigated the use of both compounds for anaerobic respiration by strain NRC-1. NRC-1 grew in CM^+ medium (containing peptone and citrate as carbon and electron sources) under strictly anaerobic conditions with either 40 mM DMSO (doubling time [t_d] = 1.2 days) (Fig. 2) or 40 mM TMAO (t_d = 1.1 days) as the sole electron acceptor. The respective respiration products dimethyl sulfide and trimethylamine accumulated concomitantly with increase in optical density. A lag in growth was observed after transfer of aerobically but not anaerobically grown cultures, indicating that components of anaerobic respiration are inducible. Microscopic examinations revealed the presence of abundant gas vesicles inside cells already during the early growth stage on DMSO or TMAO. Aerobically grown cells typically harbor abundant gas vesicles during late log and stationary phases.

The MPT cofactor of DMSO and TMAO reductases contains the transition metal molybdenum. Addition of 3 μM molybdate to the medium did not change the growth profile, indicating the presence of sufficient molybdenum in the basal salt medium. In the presence of 10 mM tungstate, a molybdate antagonist, growth on DMSO and TMAO was severely impaired (t_d of >7 days), while aerobic growth and arginine fermentation were not affected.

Construction and characterization of *dms* deletion strains. To confirm the involvement of the *dmsREABCD* operon in DMSO and TMAO respiration in *Halobacterium* sp. strain NRC-1, in-frame deletions of *dmsR*, *dmsA*, and *dmsD* were constructed. The resulting strains were designated JAM101 (Δ*dmsR* Δ*ura3*), JAM102 (Δ*dmsA* Δ*ura3*), and JAM103 (Δ*dmsD* Δ*ura3*) and tested for their ability to grow by anaer-

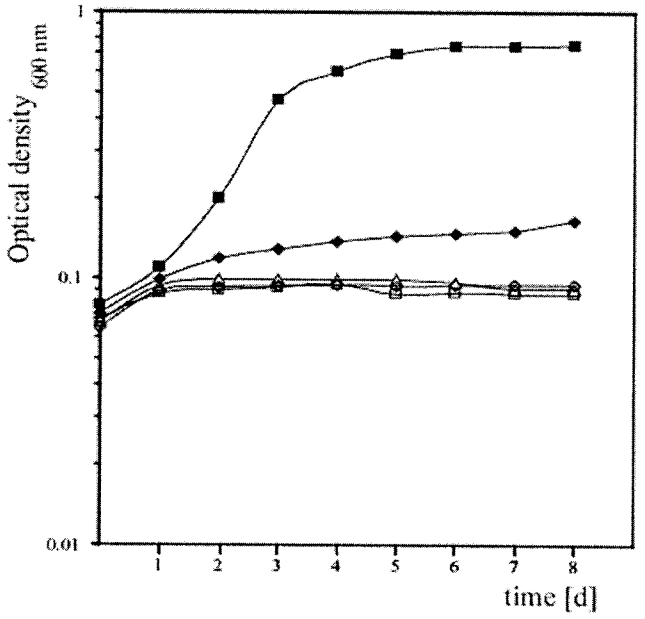

FIG. 2. Test for anaerobic growth of *Halobacterium* sp. wild-type strain NRC-1 and *dms* deletion strains on DMSO (40 mM). Incubation was at 42°C with shaking at 200 rpm. Cultures were inoculated with cells grown on L-arginine (0.5%, wt/vol). The increase in optical density was measured at 600 nm. Closed squares, NRC-1; closed diamonds, JAM101 (Δ*dmsR*); closed triangles, JAM102 (Δ*dmsA*); open squares, JAM103 (Δ*dmsD*); open diamonds, NRC-1 without DMSO in the medium.

obic respiration. Strains JAM102 (Δ*dmsA* Δ*ura3*) and JAM103 (Δ*dmsD* Δ*ura3*) failed to grow on either DMSO (Fig. 2) or TMAO (not shown), while strain JAM101 (Δ*dmsR* Δ*ura3*) displayed a marked decrease in growth on DMSO and TMAO. During anaerobic fermentation of arginine and under aerobic conditions, the growth of the mutant strains was similar to that of the wild type (data not shown). These results clearly demonstrate that the *dmsR*, *dmsA*, and *dmsD* genes of *Halobacterium* sp. strain NRC-1 are essential for anaerobic growth with DMSO and TMAO as terminal electron acceptors. The finding of a DMSO- and TMAO-negative phenotype for the *dmsR* mutant was unexpected and indicated, together with bioinformatics analysis, that this gene encodes an activator regulating transcription of the *dms* genes (see below).

Transcriptional organization of the *dms* gene cluster. To study the transcriptional organization of the *dms* gene cluster, RT-PCR analysis was performed with primer pairs that were designed to detect the *dmsR* transcript as well as cotranscription of adjacent genes. RT-PCR products were obtained for the intergenic regions of *dmsE* and *dmsA*, *dmsA* and *dmsB*, *dmsB* and *dmsC*, and *dmsC* and *dmsD* (Fig. 3). The RNA-specific recovery of these products demonstrates that the *dmsEABCD* genes are transcribed as a polycistronic unit and constitute an operon. No RT-PCR product was obtained for the intergenic region of *dmsR* and *dmsA*, indicating that *dmsR*, the putative activator, is transcribed separately.

Microarray analysis. To study *dms* gene expression and to obtain insight into the effect of anaerobic respiration on global gene expression, we compared the transcriptomes of TMAO-grown and aerobically grown cells of strain NRC-1 by using whole-genome oligonucleotide microarrays. In order to limit the effect of biological variability on the data, RNA preparations from three separately grown, comparably large quantities of cells were pooled to equal parts and fractions thereof were used for cDNA synthesis. The microarray data obtained was assessed to be of high quality based on the following criteria. Per array, only 10 to 15 features out of 8,455 total analyzed features had to be discarded as outliers due to background noise or nonuniform spot morphology. Features replicated within a single array showed low differences in absolute processed signal intensities (9% on average), and the spot-to-spot variation for replicate experiments was 11%. Green and red fluorescent signal intensities had a dynamic range in excess of 3 orders of magnitude, allowing simultaneous analysis of low- and high-intensity features. In the comparison of RNA samples derived from cultures grown under aerobic conditions, only one ORF (VNG725) displayed an expression change of greater than 1.8-fold (Fig. 4A). For the transcriptome comparison between anaerobic respiration and aerobic respiration, a gene was considered to be differentially expressed when the absolute value of the average log ratio was at least 0.3 (twofold expression change), the average log ratio error was <0.1, and the average P value of the log ratio was $<10^{-5}$ ($\sim$21% of all probes had a low P value of $<10^{-5}$).

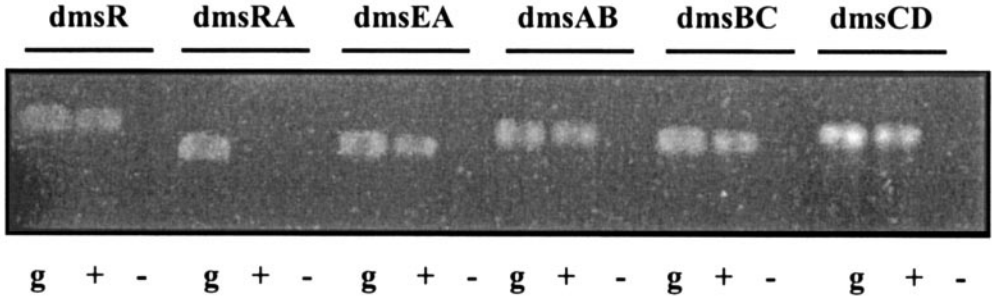

FIG. 3. RT-PCR analysis of the *dms* operon in *Halobacterium* sp. strain NRC-1. Agarose gel electrophoresis of RT-PCR assays with primers targeting *dmsR* and intergenic regions of *dmsR* and *dmsE*, *dmsE* and *dmsA*, *dmsA* and *dmsB*, *dmsB* and *dmsC*, and *dmsC* and *dmsD* is shown. g, genomic DNA as template; +, RT-PCR assays with RNA as template and conducted with reverse transcriptase; −, RT-PCR assays with RNA as template and conducted without reverse transcriptase. Sizes of products were as predicted (for *dmsR*, 384 bp; for *dmsRA*, 544 bp; for *dmsEA*, 386 bp; for *dmsAB*, 415 bp; for *dmsBC*, 454 bp; and for *dmsCD*, 374 bp).

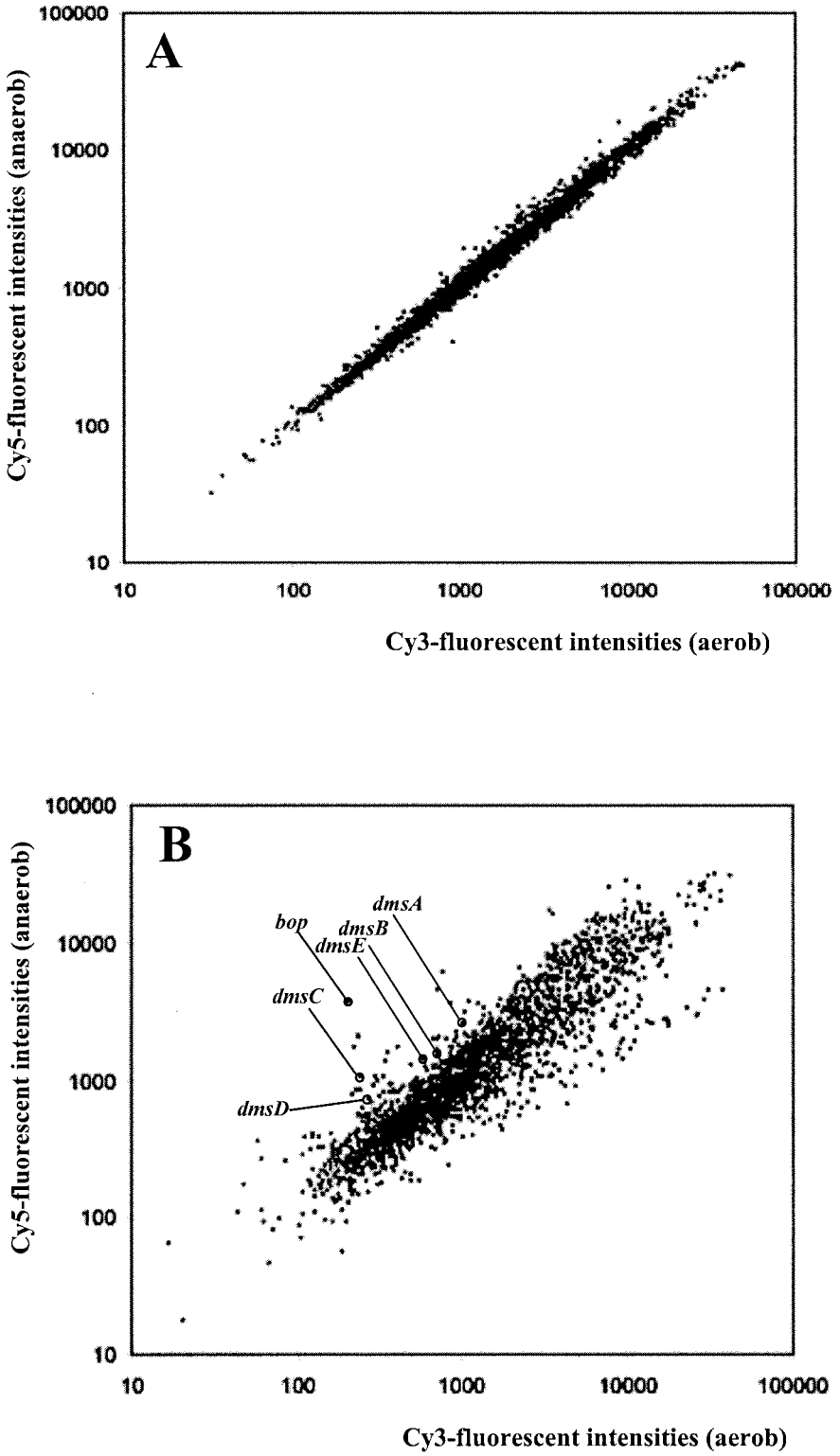

FIG. 4. Scatter plots of fluorescence intensities of Cy3-labeled cDNA versus Cy5-labeled cDNA. (A) cDNA versus cDNA derived from two cultures grown under aerobic conditions in the dark. (B) cDNA versus cDNA from three cultures, each grown by aerobic and anaerobic respiration.

Of the 2,473 ORFs of *Halobacterium* sp. strain NRC-1 represented on the array, 104 were up-regulated and 137 were down-regulated at least twofold during anaerobic respiration. To obtain an overview, differentially expressed genes were sorted according to functional categories (Table 2) (for a list of the log ratios for all ORFs, see the supplemental material). Of the 109 genes of strain NRC-1 predicted to be involved in energy metabolism, 24 genes (22%) were differentially ex-

TABLE 2. Functional categories of genes differentially expressed during TMAO respiration

Functional category	No. of genes	Anaerobic respiration vs aerobic respiration	
		Genes up-regulated	Genes down-regulated
Energy metabolism	109	11	13
Amino acid metabolism	123	2	6
Carbohydrate and lipid metabolism	89	0	6
Cofactor and secondary metabolite metabolism	128	0	8
Nucleotide metabolism	72	0	8
DNA metabolism	112	3	8
Transcription and regulation	167	6	7
Translation	152	0	47
Cellular processes	270	8	9
Transport	126	2	9
General function prediction only	51	0	1
Unknown	1,031	72	20

pressed during anaerobic respiration. Transcription of the *dmsEABCD* genes was induced approximately threefold during growth on TMAO (Fig. 4B). The *dmsR* gene was up-regulated 1.5-fold. The level of up-regulation of the *dmsEABCD* genes ranked among the highest of all differentially expressed ORFs, consistent with the requirement for these genes during anaerobic respiration.

The bacterio-opsin gene *bop* displayed the highest up-regulation (15-fold) of all ORFs. The strong differential expression of the *bop* gene is consistent with its regulation by the oxygen- or redox-sensing activator Bat (2, 3, 40, 41). Genes involved in aerobic respiration in NRC-1 were not down-regulated in the absence of oxygen. NRC-1 contains genes for three different cytochrome oxidases: *cbaABD* (VNG2193, VNG2195, and VNG2196) (orthologous with the aberrant ba_3-type cytochrome oxidases of *Natronobacterium pharaonis* and *Thermus thermophilus*), *coxABC* (aa_3-type cytochrome oxidase [11]), and *cydAB* (orthologous with quinol *bd* oxidase of *Azotobacter vinelandii*). Interestingly, the *cbaABD* genes were markedly up-regulated (fivefold) under anaerobic conditions, suggesting an unusual requirement of this cytochrome oxidase under anoxic conditions (see Discussion). The *cox* and *cyd* genes as well as other genes encoding for respiratory enzymes (e.g., equivalents to mitochondrial complex I, II, and III) were not significantly differentially expressed, indicating constitutive regulation as in *Pyrobaculum oguniense* (21) and/or their requirement during TMAO respiration (e.g., complex I and II equivalents). The transcript levels of genes involved in the citrate cycle were also not significantly differentially expressed; however, the pyruvate:ferredoxin oxidoreductase-encoding *porAB* genes, channeling carbon and electrons into the citrate cycle, were down-regulated (2.3-fold) during TMAO respiration. The ATP synthase genes were also less expressed (on average 3.3-fold) during TMAO respiration, suggesting that the ATP/ADP ratio and/or the flux rates of the ATP-ADP pools are lower in *Halobacterium* sp. strain NRC-1 during anaerobic respiration.

Congruent with the microscopic observation of abundant gas vesicles inside anaerobically grown cells, several genes encoding regulatory and structural gas vesicle proteins (*gvpED* and *gvpACNO*) were induced (two- to fivefold) during anaerobic respiration. Likewise, transcript levels of the 34 ribosomal protein genes were lower (two- to sixfold) during anaerobic respiration, which most likely reflects the altered growth rate and presumably lower ribosome content during TMAO respiration. Genes needed for MPT biosynthesis (*moaA* to *-E*, *moeAB*, *mobAB*, *modA*, *modC*/*cysU*, and *gdb*) were not significantly induced during growth on TMAO; likewise, genes involved in biosynthesis of menaquinone (*menA* to *-E*), the typical physiological electron donor for DMSO and TMAO reductases, were not differentially expressed.

Transcriptome comparison of *dmsR*$^+$ and Δ*dmsR* strains. To verify activation of the *dmsEABCD* genes by DmsR and to potentially identify additional genes regulated by DmsR, we used microarrays to compare strain JAM101 (Δ*dmsR* Δ*ura3*) against its parent, strain NRC-1 Δ*ura3*. Both strains were grown by arginine fermentation, since strain JAM101 grows only slightly on DMSO and TMAO but preliminary microarray data had shown that the *dms* operon is highly induced during growth of strain NRC-1 by arginine fermentation. As expected, the signal intensities of *dmsR* spots were substantially lower (about 50-fold) for cDNA prepared from JAM101 than for cDNA prepared from its parent strain. The *dmsE-D* structural genes were five- to eightfold less expressed in the Δ*dmsR* strain than in its parent strain. This verifies that DmsR activates transcription of *dmsEABCD*. No indication that DmsR regulates additional genes was obtained.

Bioinformatics analysis of the *dms* operon. The *dmsEABCD* genes (GC content, 67%) were found to be the only MPT oxidoreductase genes in the complete genome sequence of *Halobacterium* sp. strain NRC-1 (GC content, 68%). Identified domains and motifs of the Dms structural proteins were similar to those of other prokaryotic MPT oxidoreductases and are shown in Table 3. We also queried the unfinished genomes of *Haloarcula marismortui* and *Haloferax volcanii* for genes orthologous to the NRC-1 *dms* genes (sequence data are available at http://zdna2.umbi.umd.edu). Both genomes contain one identically organized *dms* gene cluster with 75 to 80% amino acid sequence identities of all of the deduced proteins. The reduction of DMSO and TMAO had been reported previously for both strains (23).

To examine the evolutionary relationships between haloarchaeal DmsA and members of the DMSO reductase family, an alignment was made from amino acid sequences of 90 MPT oxidoreductases and a neighbor-joining tree was constructed. A topologically representative tree containing 11 selected sequences was subsequently generated by the neighbor-joining method (Fig. 5) and by maximum-likelihood analysis. Amino acid sequence identity of DmsA from strain NRC-1 was highest with DmsA from *E. coli*, DorA from *Rhodobacter* spp., and NarG from *E. coli* and *H. marismortui* (all 21% ± 0.5% identity). Surprisingly, the topology of the phylogenetic tree suggests that haloarchael DmsA is more closely related to NarG-type nitrate reductases than to bacterial DMSO and TMAO reductases. Consistent with the phylogenetic analysis, the molybdenum atom-coordinating protein ligand of bacterial DMSO and TMAO reductases, a serine residue (7, 29, 30, 36), is not conserved; instead, a conserved aspartate residue, as in NarG of *E. coli* (4), was found in all haloarchaeal DmsA

TABLE 3. *dms* genes and Dms proteins in *Halobacterium* sp. strain NRC-1

ORF	Gene	Protein domains and motifs	Predicted protein function	COG or Pfam description
VNG826	*dmsR*	C-terminal DNA-binding domain	Regulator	COG3413, predicted DNA-binding protein
VNG828	*dmsE*		Unknown	
VNG829	*dmsA*	Leader sequence (TAT motif), vestigial [4Fe-4S] cluster binding motif, molybdopterin domain, molybdopterin-binding domain	Catalytically active subunit	COG0243, anaerobic dehydrogenases (typically selenocysteine containing)
VNG830	*dmsB*	Four iron-sulfur cluster binding motifs (ferredoxin type)	Electron transfer subunit	COG0437, Fe-S cluster-containing hydrogenase components
VNG831	*dmsC*	Leader sequence (Sec pathway), 10 predicted transmembrane helices	Membrane anchor subunit	COG5557, polysulfide reductase
VNG832	*dmsD*		Molecular chaperone	Pfam06192, cytoplasmic chaperone TorD

protein sequences. Based on the phylogenetic analysis, as well as the arrangement of cysteines in the N-terminal region, we classified haloarchaeal DmsA as a type II MPT oxidoreductase (35).

The closest homologs with known function to DmsB, DmsC, and DmsD of *Halobacterium* sp. strain NRC-1 were PsrB (40% identity) from *Wolinella succinogenes* and DmsC (16% identity) and DmsD (27% identity) from *E. coli*, respectively. Phylogenetic trees were constructed from amino acid alignments with DmsB, DmsC, DmsD, and all members of the respective cluster of orthologous genes (COG). The topology of the trees indicated that *dmsB* and *dmsD* are of archaeal evolutionary origin, while for *dmsC*, no clear correlation with the 16S rRNA phylogenetic tree was observed (data not shown). The small DmsE protein showed some identity (19%) with DorB from *Rhodobacter capsulatus*, which has been suggested to function in biogenesis of the DMSO reductase in that organism (32).

The regulator protein DmsR is predicted to harbor a helix-turn-helix DNA-binding domain in the C-terminal region, similar to that of the *bop* gene activator Bat (2) and of several predicted archaeal DNA-binding proteins (COG3413). The N-terminal region of DmsR is cysteine rich, comprising seven cysteines between Cys^{32} and Cys^{91}. Three of these cysteines, arranged as C^{82}-$X_{hydrophob}$-C-X_7-C-(P/V), were conserved in two predicted regulators of dissimilatory nitrate reductase genes (*narGH*) from the related haloarchaea *H. marismortui* (accession number AJ429077) and *H. volcanii*.

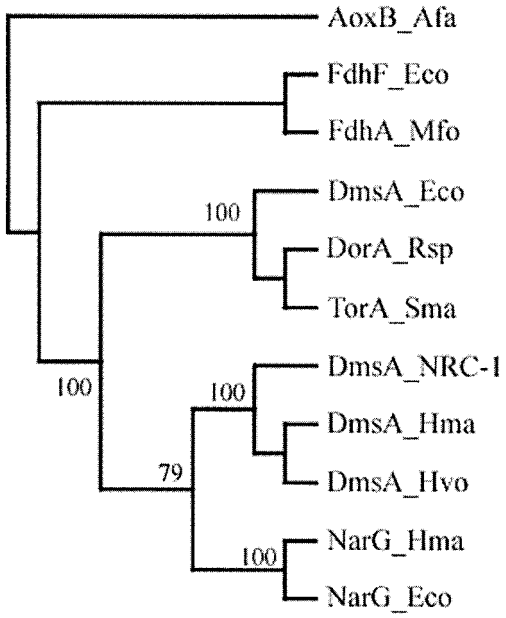

FIG. 5. Neighbor-joining tree of representative molybdopterin oxidoreductases. DmsA_Eco, *E. coli* DmsA, NP_415414; DmsA_NRC-1, *Halobacterium* sp. strain NRC-1 DmsA, NP_279804; DmsA_Hma, putative DmsA from *Haloarcula marismortui*; DmsA_Hvo, putative DmsA from *Haloferax volcanii*; DorA_Rsp, DMSO reductase from *R. sphaeroides*, AAB94874; FdhA_Mfo, formate dehydrogenase from *Methanobacterium formicicum*, P06131; FdhF_Eco, formate dehydrogenase H from *E. coli*, NP_418503; NarG_Hma, NarG from *H. marismortui*, CAD22069; TorA_Sma, TMAO reductase from *Shewanella massilia*, O87948; AoxB_Afa, arsenite oxidase from *Alcaligenes faecalis*, Q7SIF4.

DISCUSSION

The present study describes a detailed functional genomic analysis of anaerobic respiration, using DMSO and TMAO as terminal electron acceptors, in a model archaeon, *Halobacterium* sp. strain NRC-1. We employed in-frame gene deletion studies in combination with oligonucleotide microarray transcriptome analysis and physiological and phenotypic approaches to demonstrate that *Halobacterium* sp. strain NRC-1 carries a functional *dms* operon (*dmsREABCD*) as the sole system responsible for growth on either alternative electron acceptor. The *dms* structural genes are induced during anaerobic respiration. We further demonstrate that DMSO and TMAO respiration is under positive transcriptional control of a novel archaeal regulator, encoded by *dmsR*.

The DMSO reductase in strain NRC-1 is a novel member of the DMSO reductase family. Growth inhibition of DMSO or TMAO respiration by tungstate and bioinformatics analysis indicated that the catalytically active subunit, DmsA, contains molybdenum coordinated by MPT as a cofactor. Notably, DmsA of strain NRC-1 is more closely related to NarG-type dissimilatory nitrate reductases than to bacterial DMSO and TMAO reductases. Presumably, DmsA receives reducing equivalents from the iron-sulfur subunit DmsB, while both subunits are anchored to the membrane by interaction with DmsC. DmsD and possibly DmsE are involved in biogenesis in the DMSO reductase.

DmsR constitutes, along with Bat and various other archaeal proteins (e.g., a predicted regulator of *narGH* in *H. marismortui* and *H. volcanii*), a family of transcriptional regulators

(COG3413). Members of this family harbor a Bat-like helix-turn-helix DNA-binding domain (Pfam HTH 10) in the C-terminal region of the protein. In general, transcriptional activators typically harbor their DNA-binding domain in the C-terminal region (25), rendering it likely that more or even all members of COG3413 constitute transcriptional activators. The environmental signal(s) governing expression of the *dms* genes is of interest. Preliminary data from transcriptome comparisons of arginine fermentation and aerobic respiration showed that the *dms* genes are also highly induced under anaerobic conditions in the absence of both DMSO and TMAO (J. A. Müller and S. DasSarma, unpublished data). This demonstrates that the absence of the terminal electron acceptor oxygen, and not the presence of either DMSO or TMAO, is essential for induction of the *dms* genes in strain NRC-1. DmsR may respond directly to changing oxygen concentrations. The protein contains a cysteine-rich region in the N-terminal region that may be involved in metal binding (e.g., of redox-active iron) or disulfide-bridge formation. Either possibility could lead to conformational changes of DmsR, affecting DNA-binding affinity and/or interactions with other transcriptional regulators, depending on the presence or absence of molecular oxygen in the cell.

The transcriptome comparison of anaerobic and aerobic respiration provides an insight into the survival strategy of *Halobacterium* sp. strain NRC-1 in the absence of molecular oxygen. Almost all genes required for the aerobic electron transport chain have essentially the same expression level under anaerobic conditions as under aerobic conditions. This suggests that strain NRC-1 stays primed for aerobic respiration under anaerobic conditions. The observed up-regulation of the *cbaABD* genes may fit this assumption. The homologous ba_3-type cytochrome oxidase in *T. thermophilus* functions under low oxygen partial pressure (16). Assuming a similar function of the halobacterial homolog, expression of the *cbaABD* genes could enable the scavenging of molecular oxygen for use as an electron acceptor after a shift from anoxic to micro-oxic conditions. An alternative hypothesis is that the ba_3-type oxidase of strain NRC-1 may be involved in denitrification. The *T. thermophilus* enzyme is bifunctional, as it can reduce both molecular oxygen and nitric oxide (NO) (12). Although strain NRC-1 appears to be unable to grow by denitrification (Müller and DasSarma, unpublished observations), the gene products of *cbaABD* may work together with that of VNG1187, a NirK-type nitrite reductase homolog, to facilitate auxiliary energy conservation under anaerobic conditions with nitrogen oxides as electron acceptors. This strategy would be similar to the contribution of phototrophy to the energy budget of strain NRC-1. Menaquinone is presumably used both as a mobile electron carrier during aerobic respiration (28) and as an electron donor for the DMSO/TMAO reductase. The flow of electrons (and carbon) through the citrate cycle is regulated at the level of pyruvate:ferredoxin oxidoreductase and not at each individual enzyme of the cycle. This regulatory scheme could result in a fast metabolic response to the availability of oxygen as electron acceptor. Finally, the induction of *gvp* genes, resulting in increased gas vesicle formation under anaerobic conditions, would enable *Halobacterium* sp. strain NRC-1 to float to aerobic zones in the water column (40).

Our results expand the understanding of the metabolic capabilities of *Halobacterium* sp. strain NRC-1 under anaerobic conditions. Previous work utilized a combination of genetic and genomic studies to establish the purple membrane regulon, which leads to coordinate synthesis of bacterio-opsin and its chromophore, retinal, to allow for light-driven proton pumping (2, 8, 40, 41). The previous work led to the identification of a novel positive regulator, Bat, which controls the expression of the bacterio-opsin (*bop*) gene, as well as the first and last steps in the retinal biosynthetic pathway. In addition, genes involved in arginine fermentation are up-regulated at low oxygen partial pressure (26). With those results together with our results on the *dms* operon, we now know of three metabolic systems which can be induced to allow energy conservation in *Halobacterium* sp. strain NRC-1 under conditions of limited oxygen supply in the hypersaline environment.

ACKNOWLEDGMENTS

We thank Brian Berquist for helpful suggestions about the manuscript, as well as help with phylogenetic analysis, and Suraj Amonkar for help with microarray analysis. We also gratefully thank Kevin Sowers for providing access to an anaerobic glove box and Scott Vacha at Agilent Technologies for use of a microarray scanner.

This work was supported by NSF grant MCB0296017.

REFERENCES

1. **Anderson, L. A., E. McNairn, T. Luebke, R. N. Pau, and D. H. Boxer.** 2000. ModE-dependent molybdate regulation of the molybdenum cofactor operon *moa* in *Escherichia coli*. J. Bacteriol. **182:**7035–7043.
2. **Baliga, N. S., S. P. Kennedy, W. V. Ng, L. Hood, and S. DasSarma.** 2001. Genomic and genetic dissection of an archaeal regulon. Proc. Natl. Acad. Sci. USA **98:**2521–2525.
3. **Baliga, N. S., M. Pan, Y. A. Goo, E. C. Yi, D. R. Goodlett, K. Dimitrov, P. Shannon, R. Aebersold, W. V. Ng, and L. Hood.** 2002. Coordinate regulation of energy transduction modules in *Halobacterium sp*. analyzed by a global systems approach. Proc. Natl. Acad. Sci. USA **99:**14913–14918.
4. **Bertero, M. G., R. A. Rothery, M. Palak, C. Hou, D. Lim, F. Blasco, J. H. Weiner, and N. C. Strynadka.** 2003. Insights into the respiratory electron transfer pathway from the structure of nitrate reductase A. Nat. Struct. Biol. **10:**681–687.
5. **Cleveland, W. S.** 1979. Robust locally weighted regression and smoothing scatterplots. J. Am. Stat. Assoc. **74:**829–836.
6. **Cotter, P. A., and R. P. Gunsalus.** 1989. Oxygen, nitrate, and molybdenum regulation of *dmsABC* gene expression in *Escherichia coli*. J. Bacteriol. **171:** 3817–3823.
7. **Czjzek, M., J. P. Dos Santos, J. Pommier, G. Giordano, V. Méjean, and R. Haser.** 1998. Crystal structure of oxidized trimethylamine *N*-oxide reductase from *Shewanella massilia* at 2.5 Å resolution. J. Mol. Biol. **284:**435–447.
8. **DasSarma, S.** 2004. Genome sequence of an extremely halophilic archaeon, p. 383–399. *In* C. M. Fraser, T. Read, and K. E. Nelson (ed.), Microbial genomes. Humana Press, Inc., Totowa, N.J.
9. **DasSarma, S., and P. Arora.** 2002. Halophiles, p. 458–466. *In* Encyclopedia of life sciences, vol. 8. Nature Publishing Group, London, United Kingdom.
10. **DasSarma, S., and E. M. Fleischmann.** 1995. Halophiles. Cold Spring Harbor Laboratory Press, Plainview, N.Y.
11. **Denda, K., T. Fujiwara, M. Seki, M. Yoshida, Y. Fukumori, and T. Yamanaka.** 1991. Molecular cloning of the cytochrome aa_3 gene from the archaeon (archaebacterium) *Halobacterium halobium*. Biochem. Biophys. Res. Commun. **181:**316–322,
12. **Giuffre, A., G. Stubauer, P. Sarti, M. Brunori, W. G. Zumft, G. Buse, and T. Soulimane.** 1999. The heme-copper oxidases of *Thermus thermophilus* catalyze the reduction of nitric oxide: evolutionary implications. Proc. Natl. Acad. Sci. USA **96:**14718–14723.
13. **Hartman, R., H.-D. Sickinger, and D. Oesterhelt.** 1980. Anaerobic growth of halobacteria. Proc. Natl. Acad. Sci. USA **77:**3821–3825.
14. **Hughes, T. R., M. Mao, A. R. Jones, J. Burchard, M. J. Marton, K. W. Shannon, S. M. Lefkowitz, M. Ziman, J. M. Schelter, M. R. Meyer, S. Kobayashi, C. Davis, H. Dai, Y. D. He, S. B. Stephaniants, G. Cavet, W. L. Walker, A. West, E. Coffey, D. D. Shoemaker, R. Stoughton, A. P. Blanchard, S. H. Friend, and P. S. Linsley.** 2001. Expression profiling using microarrays fabricated by an ink-jet oligonucleotide synthesizer. Nat. Biotechnol. **19:**342–347.
15. **Jourlin, C., A. Bengrine, M. Chippaux, and V. Méjean.** 1996. An unorthodox sensor protein (TorS) mediates the induction of the *tor* structural genes in response to trimethylamine *N*-oxide in *Escherichia coli*. Mol. Microbiol. **20:**1297–1306.

16. **Keightley, J. A., B. H. Zimmermann, M. W. Mather, P. Springer, A. Pastuszyn, D. M. Lawrence, and J. A. Fee.** 1995. Molecular genetic and protein chemical characterization of the cytochrome ba_3 from *Thermus thermophilus* HB8. J. Biol. Chem. **270:**20345–20358.
17. **Méjean, V., C. Iobbi-Nivol, M. Lepelletier. G. Giorano, M. Chippaux, and M. C. Pascal.** 1994. TMAO anaerobic respiration in *Escherichia coli*: involvement of the *tor* operon. Mol. Microbiol. **11:**1169–1179.
18. **Miller, T. R., and R. Belas.** 2004. Dimethylsulfoniopropionate (DMSP) metabolism by *Pfiesteria*-associated *Roseobacter* spp. Appl. Environ. Microbiol. **70:**3383–3391.
19. **Mouncey, N. J., and S. Kaplan.** 1998. Redox-dependent gene regulation in *Rhodobacter sphaeroides* 2.4.1^T: effects of dimethyl sulfoxide reductase (*dor*) gene expression. J. Bacteriol. **180:**5612–5618.
20. **Ng, W. V., S. P. Kennedy, G. G. Mahairas, B. Berquist, M. Pan, H. D. Shukla, S. R. Lasky, N. S. Baliga, V. Thorsson, J. Sbrogna, S. Swartzell, D. Weir, J. Hall, T. A. Dahl, R. Welti, Y. A. Goo, B. Leithauser, K. Keller, R. Cruz, M. J. Danson, D. W. Hough, D. G. Maddocks, P. E. Jablonski, M. P. Krebs, C. M. Angevine, H. Dale, T. A. Isenbarger, R. F. Peck, M. Pohlschroder, J. L. Spudich, K. W. Jung, M. Alam, T. Freitas, S. Hou, C. J. Daniels, P. P. Dennis, A. D. Omer, H. Ebhardt, T. M. Lowe, P. Liang, M. Riley, L. Hood, and S. DasSarma.** 2000. Genome sequence of *Halobacterium* species NRC-1. Proc. Natl. Acad. Sci. USA **97:**12176–12181.
21. **Nunoura, T., Y. Sako, T. Wakagi, and A. Uchida.** 2003. Regulation of the aerobic respiratory chain in the facultatively aerobic and hyperthermophilic archaeon *Pyrobaculum oguniense*. Microbiology **149:**673–688.
22. **Oren, A.** 1991. Anaerobic growth of halophilic archaeobacteria by reduction of fumarate. J. Gen. Microbiol. **137:**1387–1390.
23. **Oren, A., and H. G. Trüper.** 1990. Anaerobic growth of halophilic archaeobacteria by reduction of dimethylsulfoxide and trimethylamine *N*-oxide. FEMS Microbiol. Lett. **70:**33–36.
24. **Peck, R. F., S. DasSarma, and M. P. Krebs.** 2000. Homologous gene knockout in the archaeon *Halobacterium salinarum* with *ura3* as a counterselectable marker. Mol. Microbiol. **35**:667–676.
25. **Perez-Rueda, E., and J. Collado-Vides.** 2000. The repertoire of DNA-binding transcriptional regulators in *Escherichia coli* K-12. Nucleic Acids Res. **28:**1838–1847.
26. **Ruepp, A., and J. Soppa.** 1996. Fermentative arginine degradation in *Halobacterium salinarium* (formerly *Halobacterium halobium*): genes, gene products, and transcripts of the *arcRACB* gene cluster. J. Bacteriol. **178:**4942–4947.
27. **Sambrook, J., E. F. Fritsch, and T. Maniatis.** 1989. Molecular cloning: a laboratory manual, 2nd ed. Cold Spring Harbor Laboratory Press, Cold Spring Harbor, N.Y.
28. **Schäfer, G., M. Engelhard, and V. Müller.** 1999. Bioenergetics of the archaea. Microbiol. Mol. Biol. Rev. **63:**570–620.
29. **Schindelin, H., C. Kisker, J. Hilton, K. V. Rajagopolan, and D. C. Rees.** 1996. Crystal structure of DMSO reductase: redox-linked changes in molybdopterin coordination. Science **272:**1615–1621.
30. **Schneider, F., J. Löwe, R. Huber, H. Schindelin, C. Kisker, and J. Knäblein.** 1996. Crystal structure of dimethyl sulfoxide reductase from *Rhodobacter capsulatus* at 1.88 Å resolution. J. Mol. Biol. **263:**53–69.
31. **Shaw, A. L. A. Hochkoeppler, P. Bonora, D. Zannoni, G. R. Hanson, and A. G. McEwan.** 1999. Characterization of DorC from *Rhodobacter capsulatus*, a *c*-type cytochrome involved in electron transfer to dimethyl sulfoxide reductase. J. Biol. Chem. **274:**9911–9914.
32. **Shaw, A. L., S. Leimkuhler, W. Klipp, G. R. Hanson, and A. G. McEwan.** 1999. Mutational analysis of the dimethylsulfoxide respiratory (*dor*) operon of *Rhodobacter capsulatus*. Microbiology **145:**1409–1420.
33. **Simon, G., V. Méjean, C. Jourlin, M. Chippaux, and M. C. Pascal.** 1994. The *torR* gene of *Escherichia coli* encodes a response regulator protein involved in the expression of the trimethylamine *N*-oxide reductase genes. J. Bacteriol. **176:**5601–5606.
34. **Thompson, J. D., T. J. Gibson, F. Plewniak, F. Jeanmougin, and D. G. Higgins.** 1997. The CLUSTAL_X windows interface: flexible strategies for multiple sequence alignment aided by quality analysis tools. Nucleic Acids Res. **25:**4876–4882.
35. **Trieber, C. A., R. A. Rothery, and J. H. Weiner.** 1996. Engineering a novel iron-sulfur cluster into the catalytic subunit of *Escherichia coli* dimethyl sulfoxide reductase. J. Biol. Chem. **271:**4620–4626.
36. **Trieber, C. A., R. A. Rothery, and J. H. Weiner.** 1996. Consequences of removal of a molybdenum ligand (DmsA-Ser-176) of *Escherichia coli* dimethyl sulfoxide reductase. J. Biol. Chem. **271:**27339–27345.
37. **Wang, G., S. K. Kennedy, S. Fasiludeen, C. Rensing, and S. DasSarma.** 2004. Arsenic resistance in *Halobacterium* sp. strain NRC-1 examined using an improved gene knockout system. J. Bacteriol. **186:**3187–3194.
38. **Wang, X., and B. Seed.** 2003. Selection of oligonucleotide probes for protein coding sequences. Bioinformatics **7:**796–802.
39. **Weiner, J. H., D. P. MacIsaac, R. E. Bishop, and T. Bilous.** 1988. Purification and properties of *Escherichia coli* dimethyl sulfoxide reductase, an iron-sulfur molybdo enzyme with broad substrate specificity. J. Bacteriol. **170:**1505–1510.
40. **Yang, C.-F., and S. DasSarma.** 1990. Transcriptional induction of purple membrane and gas vesicle synthesis in the archaebacterium *Halobacterium halobium* is blocked by a DNA gyrase inhibitor. J. Bacteriol. **172:**4118–4121.
41. **Yang, C.-F., J. M. Kim, E. Molinari, and S. DasSarma.** 1996. Genetic and topological analyses of the *bop* promoter of *Halobacterium halobium*: stimulation by DNA supercoiling and non-B-DNA structure. J. Bacteriol. **178:**84–845.
42. **Yoshimatsu, K., T. Iwasaki, and T. Fujiwara.** 2002. Sequence and electron paramagnetic resonance analyses of nitrate reductase NarGH from a denitrifying halophilic euryarchaeote *Haloarcula marismortui*. FEBS Lett. **516:**145–150.